

# COMPARISON OF TWO FAST ALGORITHMS FOR CWT COMPUTATIONS

<sup>1</sup>K. C. Ho , <sup>2</sup>Y. T. Chan

<sup>1</sup>Department of Electrical Engineering, University of Saskatchewan, SK, Canada. S7N 5A9

<sup>2</sup>Department of Electrical and Computer Engineering, Royal Military College of Canada, ON, Canada. K7K 5L0

## ABSTRACT

Continuous Wavelet Transform (CWT) is a useful technique to analyse time-varying signals. Direct computation of CWT via FFT requires  $O(N \log_2 N)$  operations per scale, where  $N$  is the data length. This paper compares two fast algorithms that compute CWT at a cost of  $O(N)$  per scale. One is à trous algorithm and the other is Shensa algorithm. Although both are based on the multiresolution analysis structure, their accuracy in computing CWT is quite different. Theoretical error expression is derived and simulation results are presented for comparison.

## I. INTRODUCTION

Most signals in practice are time-varying in nature. Analysis of these signals requires a time frequency method such as short time Fourier transform (STFT). Another time frequency technique called the wavelet transform (WT) has become popular recently because it provides a constant-Q analysis rather than constant time and frequency resolutions as in STFT. WT has been applied to many applications such as signal analysis [1], image compression [2], computer vision [3], and many others.

The continuous wavelet transform (CWT) of a signal  $s(t)$  is defined as [4]

$$\begin{aligned} \text{CWT}(a, \tau) &= \frac{1}{\sqrt{a}} \int s(t) \psi^* \left( \frac{t-\tau}{a} \right) dt \\ &= \frac{1}{\sqrt{a}} \int s(t+\tau) \psi^* \left( \frac{t}{a} \right) dt \end{aligned} \quad (1)$$

where  $\psi(t)$  is a mother wavelet function,  $a$  and  $\tau$  are the scale and translation respectively and the superscript  $*$  is complex conjugate. The signal  $s(t)$  can be reconstructed from the transform coefficients by [4]

$$s(t) = \frac{1}{C_\psi} \int_{-\infty}^{\infty} \int_{a>0} \text{CWT}(a, \tau) \frac{1}{\sqrt{a}} \psi \left( \frac{t-\tau}{a} \right) \frac{1}{a^2} da d\tau, \quad (2)$$

provided that the mother wavelet  $\psi(t)$  satisfies the admissibility condition [4]

$$C_\psi = \int_0^\infty \frac{|\Psi(\omega)|^2}{|\omega|} d\omega < \infty. \quad (3)$$

$\text{CWT}(a, \tau)$  is usually evaluated at dyadic scale  $a = 2^m$ ,  $m \geq 1$ , and sampled at  $\tau = n$ . Replacing  $\tau$  by  $n$  and expressing  $s(t)$  as a sum of its samples gives:

$$s(t) = \sum_k s(k) \text{sinc}(t-k). \quad (4)$$

Now (1) can be rewritten as

$$\text{CWT}(a, n) = \sum_k s(k+n) \psi_a^*(k) \quad (5)$$

where

$$\psi_a(k) = \frac{1}{\sqrt{a}} \int \text{sinc}(t-k) \psi \left( \frac{t}{a} \right) dt \quad (6)$$

are the samples of a bandlimited and dilated wavelet, and  $\text{sinc}(*) = \sin(\pi*)/(\pi*)$ . The coefficients  $\psi_a(k)$  can be precomputed and stored in memory. The convolution sum in (5) can be implemented by FFT. Thus computing  $\text{CWT}(a, n)$  requires  $O(N \log_2 N)$  operations per scale, where  $N$  is the data length. This is costly in most applications.

Two fast algorithms have been proposed to compute dyadic scale CWT efficiently that require only  $O(N)$  operations per scale. One is à trous algorithm [5-8] and the other is Shensa algorithm [5-6]. Both of them share the same multiresolution analysis (MRA) computational structure [9] as shown in Figure 1, but the choice of the lowpass filter  $\bar{g}$ , bandpass filter  $\bar{h}$  and the initialization filter  $q$  are different. Although the two algorithms are well known in literature, little work has been done to compare the accuracy of the two methods. The accuracy of CWT is particularly important when reconstruction from transform coefficients is needed. This paper compares the two algorithms and it is organized as follows. Section II reviews the two fast CWT algorithms. Section III studies their computation accuracy. Section IV presents simulation results and finally a brief conclusion.

## II. À TROUS ALGORITHM AND SHENSA ALGORITHM

The two algorithms are based on the MRA structure shown in Figure 1. The input signal in discrete form is first prefiltered by  $q$ . It then passes through stages of lowpass filter  $\bar{g}$  and bandpass filter  $\bar{h}$ . The bandpass filter output at stage  $m$  produces CWT at scale  $a=2^m$  and  $\tau=2^m n$ , where  $n$  is an integer. The MRA structure can be extended to provide the undecimated CWT samples [5]. For illustration purposes, we shall focus on the MRA structure only. But the results apply to the extended structure as well.

The à trous algorithm [5-8] chooses the initialization filter to be an impulse function, the bandpass filter to be the samples of a mother wavelet, and the lowpass filter  $\bar{g}$  to be à trous. That is, the impulse response of the lowpass filter  $\bar{g}(n)$  satisfies

$$\bar{g}(2n) = \delta(n)/2. \quad (7)$$

The à trous filter serves as an interpolator to interpolate the impulse responses in the bandpass filter for the missing samples in a dilated wavelet. The error in this algorithm comes from non-ideal interpolation in the à trous filter.

The Shensa algorithm, on the other hand, selects the filters such that

$$\phi(t) = 2 \sum_{l=-L'}^{L'} \bar{g}^*(l) \phi(2t+l) \quad (8)$$

$$\psi(t) = 2 \sum_{l=-L}^L \bar{h}^*(l) \phi(2t+l) \quad (9)$$

where  $2L'+1$  and  $2L+1$  are the lengths of  $\bar{g}$  and  $\bar{h}$ , and  $\phi(t)$  is the scaling function. The scaling function can be obtained by iterating (8) and detail procedures are in [4]. Equations (8)-(9) are the two-scale equations for the scaling function and the wavelet. The impulse response of the initialization filter is set to be [10]

$$q(n) = \int \text{sinc}(t) \phi^*(t-n) dt. \quad (10)$$

To design the filters for a given mother wavelet, we first select a regular lowpass filter  $\bar{g}$  and use (8) to generate the scaling function  $\phi(t)$ . Applying (10) forms the initialization filter. To fulfil (9),  $\bar{h}$  is chosen to minimize the error:

$$E = \int_{-\infty}^{\infty} |\psi^*(t) - 2 \sum_l \bar{h}(l) \phi^*(2t+l)|^2 dt \quad (11)$$

Let  $\bar{h} = [\bar{h}(-L), \bar{h}(-L+1), \dots, \bar{h}(L)]^T$  and  $\Phi(t) = 2 [\phi(2t-L), \phi(2t-L+1), \dots, \phi(2t+L)]^T$ . Taking derivative of (11) with respect to  $\bar{h}$  and setting the derivative to zero give

$$\bar{h} = \left[ \int_{-\infty}^{\infty} \Phi(t) \Phi(t)^+ dt \right]^{-1} \left[ \int_{-\infty}^{\infty} \Phi(t) \psi^*(t) dt \right]. \quad (12)$$

The error in the Shensa algorithm comes from the inexact representation of the wavelet  $\psi(t)$  by the scaling function  $\phi(t)$ .

## III. COMPUTATION ACCURACY

Since both algorithms use a common structure, we shall derive a general expression for the error square in CWT computation using the MRA structure. The accuracy of the two methods can be examined by substituting their choice of filters.

Figure 2 is the filtering path to generate the output at stage  $m$  in the MRA. Applying the downsampling identity illustrated in figure 3 gives an equivalent filtering path as shown in figure 4, where all the downsampling operations are done at the end. We use the symbol  $[\cdot]_{\uparrow \gamma}$  to denote upsampling by a factor of  $\gamma$ . That is,  $[\bar{g}]_{\uparrow 4}$  represents a filter that has 3 zeros inserted between any two samples in  $\bar{g}$ . The output before downsampling is

$$d_m(n) = \sum_k s(n-k) f(k) \quad (13)$$

where

$$f(k) = \sqrt{2^m} q * \bar{g} * [\bar{g}]_{\uparrow 2} * \dots * [\bar{g}]_{\uparrow 2^{m-2}} * [\bar{h}]_{\uparrow 2^{m-1}} \quad (14)$$

and  $*$  is the convolution operation. Ideally,  $d_m(n)$  is equal to  $\text{CWT}(2^m, n)$ . Hence using (5) the error at scale  $2^m$  is

$$\begin{aligned} \Delta(n) &= d_m(n) - \text{CWT}(2^m, n) \\ &= \sum_k s(n+k) \{ f(-k) - \psi_{2^m}^*(k) \}. \end{aligned} \quad (15)$$

To be specific, we consider a bandlimited white input signal because it contains all frequency components. As a result,  $\Delta$  becomes

$$\Delta(n) = f(n) - \psi_{2^m}^*(-n). \quad (16)$$

Taking magnitude square and summing over  $n$ , the total squared error is

$$\xi = \sum_{n=-\infty}^{\infty} |f(n) - \psi_{2^m}^*(-n)|^2. \quad (17)$$

Given a set of filters,  $f(n)$  is evaluated from (14) and the total squared error is found from (17).

The special choice of the filters in the Shensa algorithm can reduce  $\xi$  to another form. It is straightforward to show from (8) and (10),

$$q * \bar{g} = \frac{1}{2} \int \text{sinc}(t) \phi^*\left(\frac{t-n}{2}\right) dt. \quad (18)$$

Continuing the convolution process simplifies (14) to

$$f(n) = \frac{2}{\sqrt{2^m}} \int \text{sinc}(t) \sum_l \bar{h}(l) \phi^*\left(\frac{t-n}{2^{m-1}} + l\right) dt. \quad (19)$$

When  $m$  is large, (19) can be approximated by

$$f(n) \approx \frac{2}{\sqrt{2^m}} \sum_l \bar{h}(l) \phi^* \left( \frac{-n}{2^{m-1}} + l \right) \quad (20)$$

and (6) by

$$\psi_{2^m}(n) \approx \frac{1}{\sqrt{2^m}} \psi \left( \frac{n}{2^m} \right). \quad (21)$$

Hence setting  $t = n/2^m$  yields

$$\xi \approx \int_{-\infty}^{\infty} |\Psi^*(t) - 2 \sum_l \bar{h}(l) \phi^*(t+l)|^2 dt \quad (22)$$

which is the error criterion  $E$  in (11) to find the bandpass filter  $\bar{h}$ . It is therefore expected that the Shensa algorithm, in general, outperforms the à trous algorithm.

#### IV. SIMULATION

The mother wavelet was the Morlet function [1]

$$\psi(t) = \frac{1}{\sqrt{2\pi}\sigma} e^{-t^2/2\sigma^2} e^{-j2\pi f_0 t} \quad (23)$$

where  $\sigma=3$  and  $f_0=0.3$ . The signal  $s(t)$  was  $s(t)=\text{sinc}(t)$  and it had a bandwidth of 0.5. The corresponding data samples were  $s(n)=\text{sinc}(n)$ ,  $n=-128, -127, \dots, 127$ . In the à trous algorithm, the lowpass filter was  $\bar{g}=[-1, 0, 9, 16, 9, 0, -1]/32$  [5] and the bandpass filter  $\bar{h}$  was the bandlimited and dilated by two Morlet wavelet samples having a length of 49. The averaged squared error between the à trous algorithm output and the true CWT values is shown in Figure 5 for  $m=1$  to 7.

In the Shensa algorithm, the lowpass filter was a B-spline with binomial coefficients as impulse response [6]:

$$\bar{g}(n) = \frac{1}{2^r} \binom{r}{n+r/2}, \quad k = -\frac{r}{2}, -\frac{r-1}{2}, \dots, \frac{r}{2} \quad (24)$$

where  $r$  was 4 so that we had the same number of non-zero lowpass filter coefficients as in the à trous algorithm. The bandpass filter was computed from (12) with  $L=24$ . The averaged squared error in this case is also shown in Figure 5. The theoretical errors predicted by (17) was also given.

It is clear that the Shensa algorithm outperforms the à trous algorithm, giving more than 15dB improvement at moderate scale values in this particular case. In addition, the theoretical results are in close match with the simulations. Other scaling functions such as à trous and Daubechies were tested in the Shensa algorithm. The B-spline function was consistently better.

To conclude, we have examined the accuracy of CWT computation by the à trous and the Shensa algorithms. The theoretical study showed that the Shensa algorithm can choose a bandpass filter such that the squared error in CWT computation is always minimized. As a result, the Shensa algorithm in general provides a better accuracy than the à trous algorithm. The Simulation studies have verified the theoretical developments.

#### REFERENCES

- [1] O. Rioul and M. Vetterli, "Wavelets and signal processing," *IEEE Signal Processing Mag.*, vol. 8, no. 4, pp. 11-38, Oct. 1991.
- [2] M. Antonini, M. Barlaud, P. Mathieu and I. Daubechies, "Imaging coding using vector quantization in the wavelet transform domain," in *Proc. IEEE Int. Conf. Acoust., Speech, Signal Processing*, Albuquerque, NM, 1990, pp. 2297-2300.
- [3] S. Mallat, "Multifrequency channel decompositions of images and wavelet models," *IEEE Trans. Acoust., Speech, Signal Processing*, vol. 37, pp. 2091-2110, Dec. 1989.
- [4] Y. T. Chan, *Wavelet Basics*. Kluwer, 1995.
- [5] M. J. Shensa, "The discrete wavelet transform: wedding the à trous and Mallat algorithms," *IEEE Trans. Signal Processing*, vol. 40, no. 10, pp. 2464-2482, Oct. 1992.
- [6] O. Rioul and P. Duhamel, "Fast algorithms for discrete and continuous wavelet transforms," *IEEE Trans. Inform. Theory*, vol. 38, no. 2, pp. 569-586, Mar. 1992.
- [7] M. Holschneider, R. Kronland-Martinet, J. Morlet and Ph. Tchamitchian, "A real-time algorithm for signal analysis with the help of the wavelet transform," in *Wavelets, Time-Frequency Methods and Phase Space*, J. M. Combes, A. Grossmann, and Ph. Tchamitchian, Eds. Berlin: Springer, IPTI, 1989, pp. 286-297.
- [8] P. Dutilleul, "An implementation of the 'Algorithme à Trous' to compute the wavelet transform," in *Wavelets, Time-Frequency Methods and Phase Space*, J. M. Combes, A. Grossmann, and Ph. Tchamitchian, Eds. Berlin: Springer, IPTI, 1989, pp. 298-304.
- [9] S. G. Mallat, "A theory for multiresolution signal decomposition: the wavelet representation," *IEEE Trans. Pattern Analysis, Machine Intell.*, vol. 11, no. 7, pp. 673-693, July 1989.
- [10] X. G. Xia, C. C. J. Kuo and Z. Zhang, "Wavelet coefficient computation with optimal prefiltering," *IEEE Trans. Signal Processing*, vol. 42, no. 8, pp. 2191-2197, Aug. 1994.

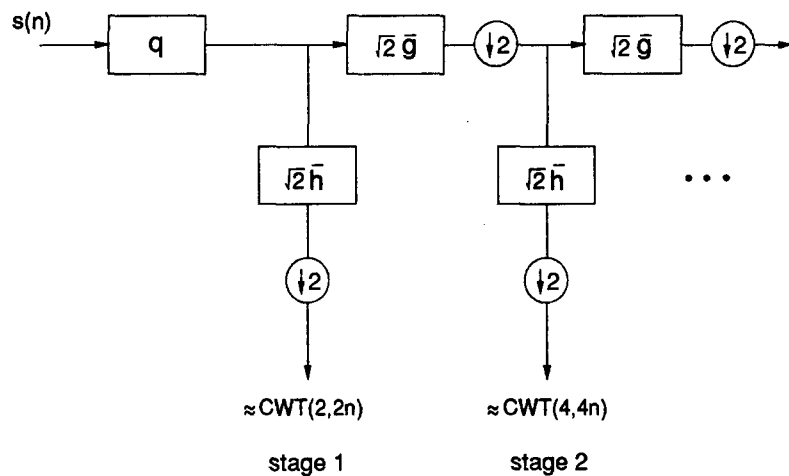


Fig. 1 The MRA structure for CWT computation

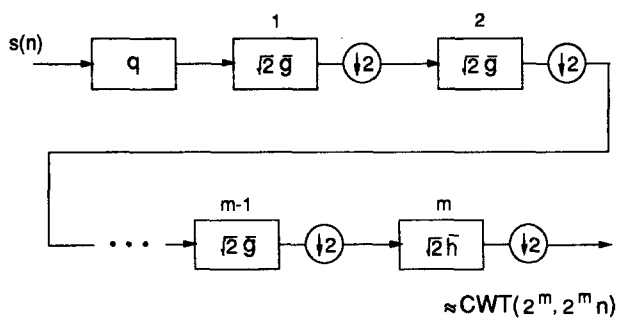


Fig. 2 The filtering path in MRA to generate output at stage  $m$

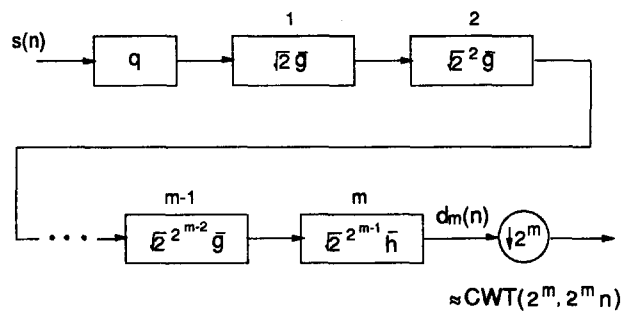


Fig. 4 An equivalence of the filtering path shown in fig. 2

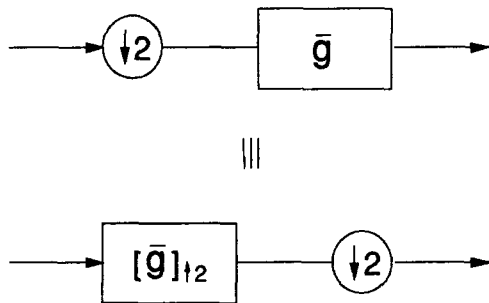


Fig. 3 A downsampling identity

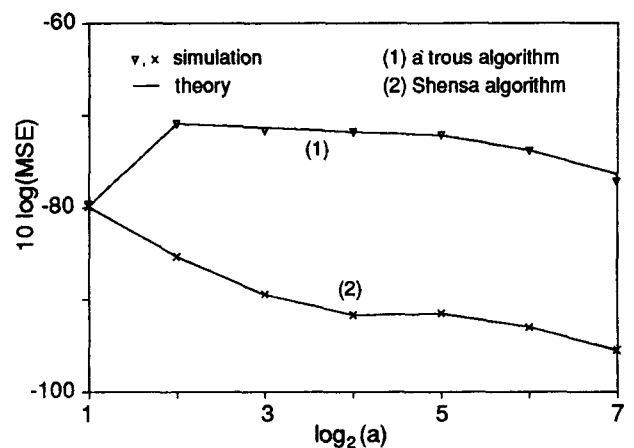


Fig. 5 Comparison of accuracy between the à trous and the Shensa algorithms